CHEMISTRY
A EUROPEAN JOURNAL

DOI: 10.1002/chem.201102137

pH-Tunable Hydrogelators for Water Purification: Structural Optimisation and Evaluation

Daniel M. Wood,[a] Barnaby W. Greenland,[a] Aaron L. Acton,[a] Francisco Rodríguez-Llansola,[b] Claire A. Murray,[a] Christine J. Cardin,[a] Juan F. Miravet,[b] Beatriu Escuder,[b] Ian W. Hamley,[a] and Wayne Hayes*[a]

Abstract: A focused library of potential hydrogelators each containing two substituted aromatic residues separated by a urea or thiourea linkage have been synthesised and characterized. Six of these novel compounds are highly efficient hydrogelators, forming gels in aqueous solution at low concentrations (0.03–0.60 wt %). Gels were formed through a pH switching methodology, by acidification of a basic solution (pH 14 to ≈4) either by addition of HCl or via the slow hydrolysis of gluco-no-δ-lactone. Frequently, gelation was accompanied by a dramatic switch in the absorption spectra of the gelators, resulting in a significant change in colour, typically from a vibrant orange to pale yellow. Each of the gels was capable of sequestering significant quantities of the aromatic cationic dye, methylene blue, from aqueous solution (up to 1.02 g of dye per gram of dry gelator). Cryo-transmission electron microscopy of two of the gels revealed an extensive network of high aspect ratio fibers. The structure of the fibers altered dramatically upon addition of 20 wt % of the dye, resulting in aggregation and significant shortening of the fibrils. This study demonstrates the feasibility for these novel gels finding application as inexpensive and effective water purification platforms.

Keywords: electron microscopy · gels · self-assembly · supramolecular chemistry · X-ray diffraction

Introduction

The design and synthesis of low molecular weight gelators (LMWG) has been a rapidly expanding field of research over the previous 15 years.[1] A typical LMWG is a molecular species that self-assembles into extended fibrillar structures from solution. Under ideal conditions, the supramolecular[2] fibrils increase in size to almost macroscopic length scales, eventually producing an interpenetrating network that percolates throughout the liquid phase, immobilizing the solvent through capillary action. Thus, small quantities of the LMWG (<1% w/v) can inhibit the flow of a large volume of solvent.[3] The design of LMWGs presents a great challenge with the success (or not) of a new gelator dependent on the subtle interplay between the relative solubility[4] of the potential gelator under different conditions (i.e., temperature or pH), coupled with the position and directionality the key residues that drive the formation the supramolecular structures during gelation. Thus, there have been a series of elegant structural optimisation studies based on a varied range of skeletal motifs as detailed in an excellent recent review on this topic.[5] Interest in these intriguing molecules is maintained as a consequence of the increasing number of practical applications for which they may be suited, spanning areas as diverse as catalysis,[6] or electronic[1b] and photonic materials.[7] Within this expanding research field is the design and synthesis of molecules that gel in aqueous conditions, so-called hydrogelators.[8] The ability to form gels from aqueous rather than organic solvents (i.e., organogels) opens exciting new opportunities, moving the field into new areas including biomaterials,[9] drug delivery[10] and water purification.[11] In a recent communication,[12] we reported the synthesis of a structurally simple urea based hydrogelator that is accessed through a one-pot synthesis from commercially available materials.[13] The gelator was readily soluble at room temperature in water under basic conditions (pH 12, NaOH), but formed gels rapidly as the aqueous solution was acidified. As the pH was reduced the system underwent a dramatic change in colour from a vivid orange solution to a pale yellow gel. In addition, the gel was found to extract large quantities of the aromatic cationic dye methylene blue from solution, demonstrating clear potential for water purification. In this paper, we report the synthesis of a family of structurally related potential gelators and evaluate their ability to form hydrogels through a pH switching protocol. Dye extraction studies, combined with rheological analysis and inspection of the solid-state structures of three of these new gelators provide new insights to

[a] D. M. Wood, Dr. B. W. Greenland, A. L. Acton, C. A. Murray, Prof. C. J. Cardin, Prof. I. W. Hamley, Dr. W. Hayes
Department of Chemistry, University of Reading
Whiteknights, Reading, RG6 6AD (United Kingdom)
Fax: (+44) 118-378-6331
E-mail: w.c.hayes@reading.ac.uk

[b] Dr. F. Rodríguez-Llansola, Prof. J. F. Miravet, Prof. B. Escuder
Departament de Química Inorgànica i Orgànica
Universitat Jaume I, Avda.Sos Baynat s/n
12071 Castelló (Spain)

Supporting information for this article is available on the WWW under http://dx.doi.org/10.1002/chem.201102137.

help guide the de novo production of these fascinating molecules.

Results and Discussion

Inspection of the structure of our recently reported gelator **1** reveals three distinct structural motifs with an aromatic nitro group (ring A) and an aromatic diacid (ring B) separated by a urea residue (C, Figure 1). To gain a better understanding of how each structural feature influences the gelation and dye extraction properties of the hydrogelator, a library of closely related compounds, differing in the number and positioning of key functional groups on the aromatic rings A and B (Figure 1) were synthesised. Production of the library was facilitated by the modular nature of the synthesis, which typically involved the addition of a commercially available aromatic amine to an isocyanate (Table 1), allowing rapid access to a series of closely related structures for further analysis. Thus, nine novel potential gelator compounds were synthesised (**1**–**9**). For the majority of cases (**1**–**5**), synthesis was achieved in a high yield (> 84%) via addition of either 5-amino isophthalic acid (**10**) or 4-aminobenzoic acid (**11**) to an aromatic isocyanate (**12**–**15**). The five novel urea compounds produced via this route differed by the inclusion and relative positions of the nitro group on ring A of the molecule (**1**, **3**, **4** and **5**) and the number and position of carboxylic acid groups on the B ring of the molecules (**1** and **3**). Attempts to access thiourea **7** and nitrile **8** through the one-pot route resulted in the formation of multiple products (as determined by ^{1}H NMR spectroscopic analysis), from which the desired product could not be isolated in a pure form. It was found, however, that the formation of side-

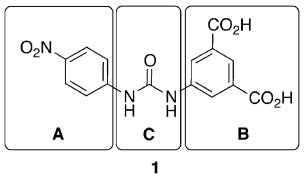

1

Figure 1. Structure of urea **1** highlighting the three distinct potential recognition motifs contained within the low molecular weight hydrogelator.

Table 1. Synthesis of potential low molecular weight hydrogelators.[a]

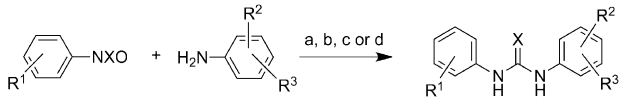

Isocyanate	Aromatic amine	Conditions/Overall yield [%]	Product
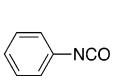 12	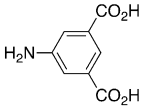 10	a/95	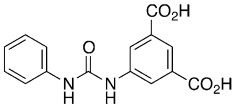 2
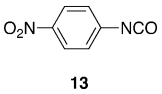 13	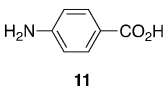 11	a/84	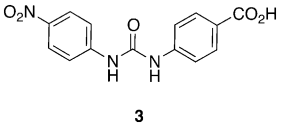 3
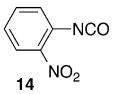 14	**10**	a/85	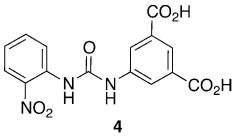 4
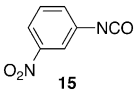 15	**10**	a/92	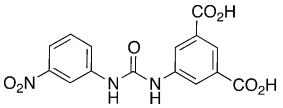 5
13	**10**	a/93	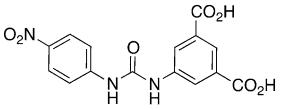 1
13	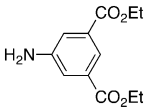 16	b/28	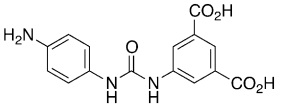 6
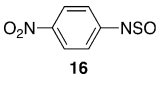 16	**16**	c/86	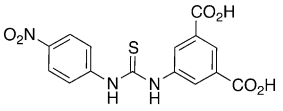 7
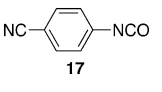 17	**16**	d/62	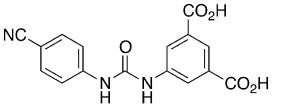 8
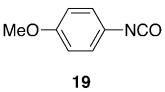 19	**10**	a/26	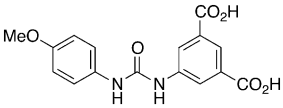 9

[a] Reaction conditions: a) THF, RT, 24 h; b) 1) THF, RT, 24 h; 2) EtOH/EtOAc, H_2, Pd/C, RT, 1 h; THF/H_2O, KOH, RT, 24 h; c) 1) THF, RT, 24 h; 2) THF/H_2O, KOH, RT, 24 h; d) 1) THF, RT, 24 h; 2) THF/H_2O, LiOH, RT, 24 h.

products could be suppressed by addition of the known[14] aromatic amino-diethyl ester, **16** to either the aromatic isocyanate **13** or isothiocyanate **17**, followed by saponification to deliver the targeted diacids **7** and **8**. To expand the library of potential gelators further, a palladium-catalysed reduction of thenitro group on **1** afforded aniline **6**. It was thought that the interchange of the hydrogen-bond accepting nitro group for a hydrogen bond donor such as the amine group would provide further insight into the nature of the self-assembled supramolecular gels formed by this class of material.

Gelation studies by pH switching: The relative gel-forming potential of each of the novel compounds was assessed initially by the operationally simple tube inversion test. In many gel studies, this is achieved through heating a known quantity of the potential gelator in a solvent to form a homogeneous solution. Subsequent cooling of the solution allows the formation of the gel-state product. This method was not found to be appropriate in order to assess the performance of these potential hydrogelators (**1**–**9**) as a consequence of the poor solubility that they exhibit in pure water even at elevated temperature. It was found, however, that all nine potential gelators were readily soluble in basic solutions (NaOH 0.2 M, pH 13). Subsequent acidification of the homogeneous solutions either by the addition of HCl or by using the robust glucono-δ-lactone protocol introduced by Adams' group[15] resulted in rapid (i.e., less than 1 h) homogeneous gel formation for solutions of six of the potential gelator molecules (**1**, **3**–**5**, **7** and **8**, Table 3). The compounds without an electron-withdrawing group on the A ring of the urea (that is **2**, **6** and **9**) did not to produce a stable gel under these conditions (gelation studies were carried out up to 50 mM). These results demonstrate the critical importance of a group that has hydrogen bond accepting ability in promoting gelation. Through the employment of the glucono-δ-lactone pH switching methodology, the critical gelation concentration (cgc) was established between 0.9 and 20 mM for the six gelating molecules. As a consequence of the extremely low molecular weight of these compounds (each under 400 Da) all six molecules are "super gelators",[3] forming stable gels below 1% w/v under these experimental conditions. The cgc for hydrogelator **1** (0.03% w/v) is amongst the lowest reported to date. Comparison of the mono acid gelator **3** and diacid gelator **1** reveals that the cgc values differ by over twenty times (20 and 0.9 mM, respectively), demonstrating the importance of both of the two acids of **1** in maintaining the supramolecular gel structure. The cgc values for the isomeric series **4**, **5** and **1** where the nitro group is positioned at the *ortho*, *meta* or *para* position of the "A" aromatic ring decreases the cgc by over an order of magnitude (17 to 0.9 mM, respectively). These results clearly show that successful gel formation was equally dependent on the relative directionality of the hydrogen-bond motifs on both the aromatic rings and the total number of hydrogen-bond donors and acceptors. Exchange of the *ortho* nitro group for a nitrile residue (compare **1** and **8**), or replacement of the urea with a thiourea (compare **1** and **7**) also resulted in a small increase in the cgc value in both examples. It is interesting to note that whilst the hydrogels formed from **1**, **3**, **7** and **8** were stable over long time periods (degradation was not observed over several weeks), the gels formed from **4** and **5** (*ortho* and *meta* nitro species, respectively) formed crystal-like structures a few hours after the initial gelation, resulting in a breakdown in the integrity of the gel (Figure 2). Intriguingly, gel metastability[16] was only observed when gelation was induced slowly through the hydrolysis of glucono-δ-lactone rather than if the gel was formed quickly through direct addition of HCl (where gels remained indefinitely stable). This observation suggests that the kinetics of gel formation may play a key role in determining the longevity of the resulting hydrogel, although clearly many other factors including salt type and concentration will vary between the gels formed through the two pH switching methods. To investigate the stability of all the hydrogels in detail, thermal response studies of the gels were performed (Table 3 20 mM, glucono-δ-lactone pH switching method). Vials containing the gels were immersed in an oil bath and the temperature was increased to 100 °C over about 1 h whilst the gel stability assessed by the tube inversion test at 5 °C intervals. Comparison of the stability results

Table 2. Results of gelation studies via the tube inversion test for the novel ureas **1**–**9**.

Compound	Observation	cgc [mM]	wt% gel
2	precipitate		
3	gel	20	0.60
4	gel	17	0.16
5	gel	4.5	0.56
1	gel	0.9	0.03
6	precipitate		
7	gel	2.7	0.10
8	gel	4.6	0.15
9	precipitate		

Table 3. Thermal stability study of the hydrogels assessed by the tube inversion test for gels. All gels were formed via the glucono-δ-lactone pH switching method (20 mM).

Gelator	T [°C] failed inversion test	T [°C] precipitate formed
1	>100[a]	>100
3	70	70
4	40	42
5	60	61
7	65	70
8	40	43

[a] At 85 °C **1** visibly released water forming a layer above the gel, however the gel remained stable upon inversion up to 100 °C.

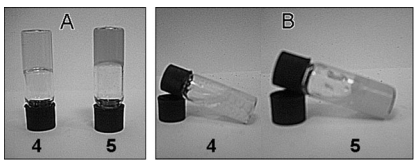

Figure 2. Tube inversion tests for gels formed from **4** and **5** at A) $t=1$ h and B) $t=6$ h. For a colour image see the Supporting Information.

for the isomeric series of gels **1**, **4** and **5** reveals a close correlation with the cgc values exhibited by the gels. The *para*-nitro gelator **1** remained stable when held at the boiling point of water,[17] whereas the *ortho*- (**4**) and *meta*-nitro (**5**) gels failed the tube inversion test at 40 and 60 °C, respectively. Intriguingly, failure of gels **4** and **5** was accompanied by subsequent precipitation from solution. This trend for gel dispersion and precipitation was observed for each of the remaining hydrogels which were all stable at elevated temperatures ranging from 40 and 70 °C. Despite solvent constraints preventing the precipitation of hydrogel **1** from being observed, these results indicate that metastability[16] may be a general feature of all these structurally related gels.

Gelation through pH switching and UV/Vis absorption studies: Whilst conducting the gelation experiments it became apparent that several of the compounds underwent a dramatic colour change as the pH was lowered to produce the gel state, typically changing from a vibrant orange to a pale yellow (see Figure 3, inset, and Supporting Information).

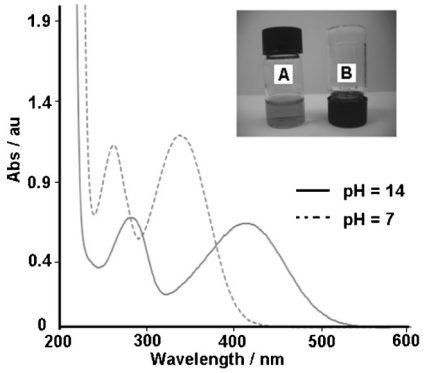

Figure 3. UV/Vis spectra (water with 10% DMSO v/v), for a solution of gelator **3** at pH 14 and pH 7 (concentration for both solutions = 1 mg mL^{-1}). Photo inset: Vial A, solution of **3** at pH 14, vial B, hydrogel **3** at pH 1. For a colour image see the Supporting Information.

Absorbance bands for the gelators in basic solutions (pH 14, NaOH in water) may be determined readily by UV/Vis spectroscopy, whereas similar absorbance measurements under acidic conditions were hindered by scattering caused by the gel, which spontaneously forms at low pH. To overcome this problem, neutral solutions (pH 7) of gelator were prepared by gentle heating of 1 mg of gelator in 10 mL of water and 10% DMSO (v/v). Under these conditions, the gelators remained soluble allowing for accurate determination of the absorbance bands (exemplified for **3** in Figure 3, see Supporting Information for spectra for other compounds). UV/Vis data under basic and neutral conditions for all six hydrogelators are summarised in Table 4. From Table 4 it can be seen that five of the six gelators exhibit significant differences in λ_{max} in solution at pH 14 when compared to that at neutral pH. It should be noted, however, that the nitrile gelator **8** appears colourless under both pH regimes as all appreciable absorbance bands fall outside the visible spectrum. This behaviour is reasonable considering the different electronic properties of nitrile and nitro substituents. For example, the maximum absorbance of nitrobenzene is considerably red-shifted when compared to that of benzonitrile (λ_{max} values for the K band are 251 and 224 nm, respectively).[18]

Table 4. λ_{max} at pH 14 and pH 7 for solutions containing gelators **1**, **3**–**5**, **7**, **8** (water with 10% DMSO v/v, 0.3 mM).

Gelator	λ_{max} [nm] at pH 14	λ_{max} [nm] at pH 7	Shift in λ_{max} [nm]
3	418	345	−75
4	440	414	−26
5	350	350	0
1	419	343	−76
7	386	371	−15
8	314	285	−29

Gel rheology studies: Mechanical studies of the six new gels at constant concentration (20 mM) were performed using a cone and plate rheometer with a shear frequency sweep at 1.0% strain to determine how structural variations impacted on their macroscopic rheological characteristics. All of gels exhibited similar rheological profiles and behave as typical Bingham fluids (exemplified for nitrile gel **8** in Figure 4 and in Table 5). Each gel was observed to have a storage modulus (G′) that was essentially independent of the shear rate above a certain threshold. In addition, all of the gels except **5**, exhibited a value of G′ that was between one and two orders of magnitude greater than G″. Comparison of the measured values for G′ and G″ (Table 5) with the cgc parameters for these gels (Table 2) reveals little correlation between these two properties within this series of gelators.

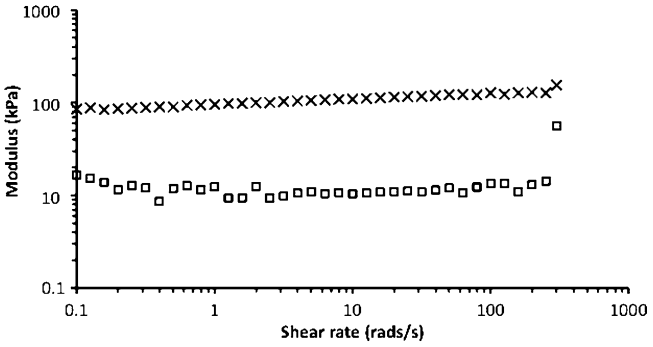

Figure 4. Rheological data for nitrile gel **8** (20 mM) in water, G′: ×, G″: □.

Table 5. Maximum storage and loss moduli for the hydrogels.

Gelator	Maximum G′ [kPa]	Maximum G″ [kPa]
3	84.2	1.4
4	166	7.1
5	359	23.6
1	294	31.9
7	34.4	4.6
8	123	13.4

This can be exemplified by comparison of G′ for the nitro-substituted gelators **1** and **5**, the *para*-substituted gelator **1** possesses the lower cgc value, yet the *meta* nitro substituted gelator **5** formed the physically more robust gel.

Methylene blue absorption studies: To facilitate the study of contaminant extraction from aqueous media, initial experiments were conducted by measuring the dye uptake of the novel gelator compounds from aqueous solutions.[11,12,19] The advantage of using a dye with a high absorption coefficient for these experiments is that the relative efficiencies of the gelators can be quantified easily by UV/Vis absorption studies, or even by visual inspection. For these specific gelators, this process is facilitated by fact that the maxima in the adsorption bands for the gelators occur between 285 and 414 nm (see Table 4), far removed that of methylene blue which exhibits a $\lambda_{max} = 667$ nm, allowing simple determination of the relative dye uptake of the gelators. This process is exemplified in Figure 5 which shows photographs of methylene blue removal for the three isomeric nitro-diacid derivatives **1**, **4**, and **5** after 48 h. In contrast to previously reported results, experiments were conducted by addition the preformed gel (1 mL, 20 mM) to a solution of methylene blue that was stirred gently (for a time lapse video of a typical experiment see Supporting Information). Comparison with the control sample, where the gelator was not added clearly shows that all three gels were capable of extracting dye from aqueous solutions. Dye uptake was quantified by analysis of the absorbance band at 667 nm in the UV/Vis absorption spectra of the four solutions which confirms that the relative absorbance efficiencies were 70% (**4**), 87% (**5**) and >99% (**1**), respectively. To measure the kinetics of dye extraction by the gelators, a time dependent dye uptake experiment was conducted. For each compound, 1 mL of the hydrogel (20 mM, pH 1, ~7 mg) was added to a stirred solution of aqueous methylene blue solution (100 mL, 8 mg L^{-1}) and the concentration of dye remaining in solution was measured periodically over 280 min by UV/Vis spectroscopy (exemplified for a typical experiment using *para*-nitro urea gelator **1**, Figure 6A). A plot of the λ_{max} (667 nm) as a function of time for all six gelators (Figure 6B: **1**, **4** and **5** and C: **3**, **7** and **8**) reveals a significant difference in both the maximum dye uptake for the gelators and the relative rates of dye extraction. Analogous studies for **1** (prior to gel formation) and **9** (both prior to and post gel formation) revealed dye uptake values of 28, 28 and 49%, respectively (see Figure S13 in the Supporting Information). Comparison of the dye extraction rates for the isomeric gelators **1**, **4** and **5** revealed that whereas the *ortho* and *meta*-nitro substituted gels reached saturation within the timescale of the experiment, exhibiting a maximum dye uptake of 34 and 50% for

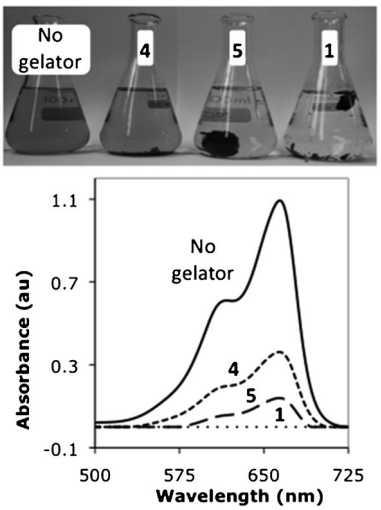

Figure 5. Top: Photograph of a solution of methylene blue (8 mg mL^{-1}) and flasks containing the same initial concentration 48 h after addition of the pre formed gels (1 mL, 20 mM) of **4**, **5** or **1** (left to right, respectively). Bottom: UV/Vis spectra of a filtered sample of the solution from each of the flasks. For a colour image see the Supporting Information.

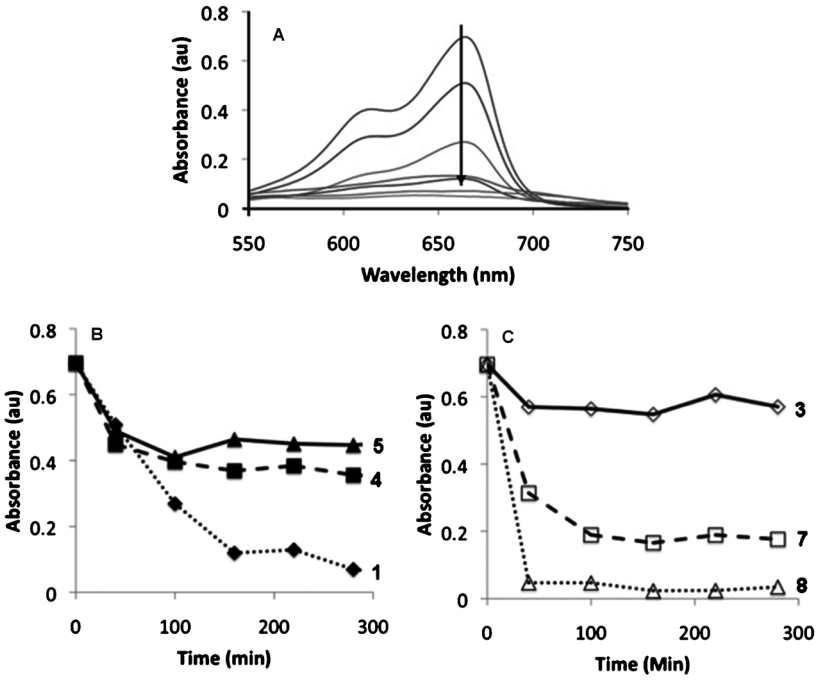

Figure 6. Plot A: UV/Vis absorption spectra a stirred solution of aqueous methylene blue (100 mL, 8 mg L^{-1}) up to 280 min after addition of 1 mL of the hydrogel **1** (20 mM, ~7 mg). Plots B and C: λ_{max} (667 nm) for the methylene blue absorption in solution (100 mL, 8 mg L^{-1}) up to 280 min after addition of gels.

4 and **5**, respectively, the *para*-nitro gel **1** extracted essentially all of the dye from solution (98%). Under the same conditions mono acid gelator **3** was the least effective at dye extraction (28%), whilst the gelators with the nitrile (**8**) and thiourea gelators (**7**) extracted 98 and 79% of the dye, respectively. Although the maximum dye absorption for gels **1** and **8** was similar (>98%), the nitrile gelator (**8**) reached this level of dye extraction after a period of only 20 min, when compared to 280 min for the nitro-substituted gelator **1**. Table 6 shows the quantity of dye sequestered by the pre-formed hydrogels after addition to stirred solutions of an excess of methylene blue. The maximum absorbed by the gels varied widely from approximately 4 wt% dye uptake (**4**) to over 100 wt% (1000 mg g^{-1}) dye uptake (**1** and **8**). These values may be compared to those for previously reported hydrogelators such as the tripeptide produced by Banerjee and co-workers, which exhibited a maximum uptake of 10.6 mg g^{-1} of the dye rhodamine red from water.[11]

Table 6. Maximum absorption of methylene blue dye from water by preformed hydrogels.

Gelator	Weight dye uptake [mg g^{-1}]	Dye uptake per molecule of gelator [mol mol^{-1}]
3	37	0.03
4	39	0.04
5	58	0.05
1	1020	1.1
7	88	0.08
8	1020	1.1

Hydrogel analysis by cryo-transmission electron microscopy (TEM): Cryo-TEM has become an increasing important analysis technique for the study of gels. The vitrification of the solvated gel prior to analysis retains the nanoscale structure in its native hydrated-state, providing valuable insights into the self-assembled structures of the unperturbed hydrogel.[20] The technique has been used extensively to study peptidic gelators,[21] but less frequently to image non-biologically inspired hydrogelators.[22] Figure 7A and B show cryo-TEM images for the *para*-nitro (**1**) and nitrile (**8**) gels that exhibited the maximum dye uptake values within these studies. Both gels exhibit an extended network consisting of high aspect ratio fibers each of which measured approximately 8 nm wide and fiber lengths extending over 10 μm in length. Cryo-TEM analysis of a sample of gel **8** containing 20 wt% dye revealed a dramatic change in the appearance of the fibrils (Figure 7C, see Figure 7D for a photograph of the dye containing gel). Inclusion of the dye caused a significant decrease in the length of the fibers to approximately 600 nm. In addition there is clear evidence for aggregation of the fibers, with the resulting bundles exhibiting a width of up to 50 nm. It is apparent, however, that gelator **8** is sufficiently robust in order to maintain its extended network during preparation for cryo-TEM in the absence of the dye (see Figure 7B), thus inclusion of methylene blue within the fibrils must at least have an impact on the strength of the fibrils.

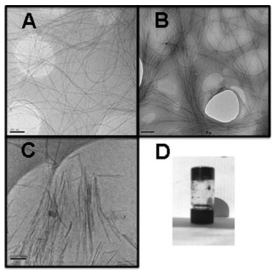

Figure 7. Cryo-TEM images of hydrogels: A) **1**, 20 mM; B) **8**, 20 mM, C) **8** (20 mM) containing 20 wt% methylene blue. D) Tube inversion test of the gel **8** (20 mM) containing 20 wt% methylene blue. All gels formed through the glucono-δ-lactone pH switching methodology, scale bars on TEM images all 200 nm. For a colour image see the Supporting Information.

Solid-state analysis: In order to gain an insight into the molecular ordering within the gel networks, differential scanning calorimetry (DSC) of the xerogel forms of the hydrogels was conducted. In all cases, the first heating ramp of the DSC exhibited multiple thermal events, which were not apparent in the second heating ramp (see Figure S9A to F for thermograms). Analysis of the complex DSC traces was hindered by the composition of the residual mass which contained the gelator, glucono-δ-lactone and NaOH (see Figure S9G for the thermogram)—the latter two components were required to effect hydrogel formation via the pH switching methodology. The dye uptake characteristics of the hydrogel materials could potentially be related to the corresponding solid-state structures. Previous solid state structural analysis of *para*-nitro hydrogelator **1**[12] revealed a highly ordered and regular array with ribbons of strictly planar molecules connected via nitro to urea hydrogen bonds[23] which were incorporated into extended two dimensional layers through dimerisation of the carboxylic acid groups. Solid-state analysis of the mono-acid gelator **3** did not reveal such a regular extended array (Figure 8). In the solid state **3** is evident as discrete dimers maintained via carboxylic acid hydrogen bonds (O-H···O, 180°, 2.62 Å, Figure 8). Each dimer was incorporated into a higher ordered solvated array through hydrogen bonding to protic solvent. The methanol molecules permit indirect nitro to urea links (OH···ON 169±8°, 2.95±0.09 Å, N-H··· O-N, 159° ±3, 2.93±0.04 Å, because $Z'=2$,[24] the range includes the values for the two distinct molecules in each asymmetric unit). The solid state structure of the *meta*-nitro gelator **5** also contains two molecules in the asymmetric unit ($Z'=2$, Figure 9). Each molecule adopts a highly twisted conformation, with the two aromatic rings offset by 47 and 63° (Figure 9). Tapes were evident that consisted of alternating bifurcated urea hydrogen bonding and N-H$_{urea}$···O-N interactions. These tapes are, in turn, connected via carboxylic acid dimers (4 distinct hydrogen bonds all within the range O-H···O, 174±3°, 2.62±0.03 Å). Thus, in contrast to **1**, both mono acid **3** and *meta* nitro-compound **5** do not possess such a dramatic extended layered aromatic surface in the solid state that is suitable for efficient dye uptake.

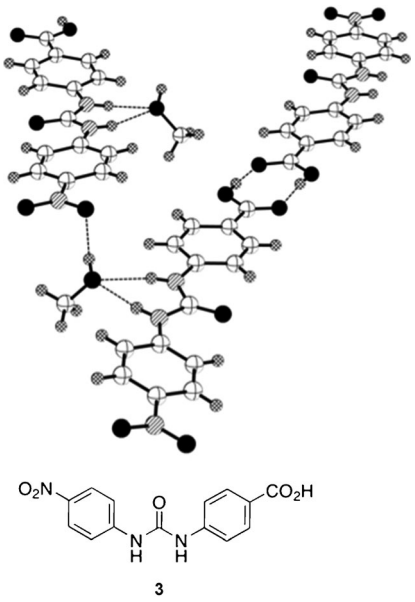

Figure 8. Top: Solid-state structure of hydrogelator **3** revealing a discrete hydrogen bonded dimer and the role of the methanol within the crystal lattice.

Conclusion

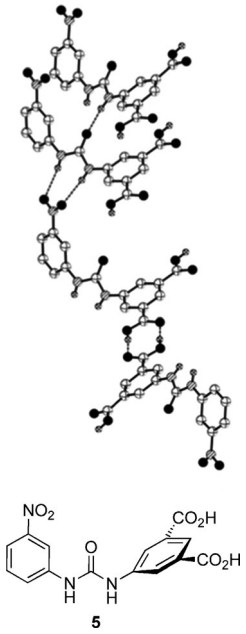

Figure 9. Solid-state structure of hydrogelator **5** showing the three dominant hydrogen bonding interactions of urea–urea, nitro-urea and carboxylic acid dimerisation (in both cases the non-hydrogen bonding hydrogen atoms removed for clarity).

A library of structurally related and synthetically accessible hydrogelators has been synthesised and characterized. Gelation was induced by acidification of a basic solution of the small molecule gelator either by addition of HCl or by the slow hydrolysis of glucono-δ-lactone. The most efficient gelator produced hydrogels at an extremely low cgc values (ca. 0.03 wt%). Frequently, gelation occurred with a concomitant colour change from deep orange to pale yellow which was measured by UV/Vis spectrometry and could be observed visually. Hydrogelators **4** and **5** were found to be metastable when formed slowly under glucono-δ-lactone hydrolysis conditions, but generated a highly stable hydrogel with lifetimes of several weeks when formed rapidly by addition of HCl to the basic solution. All of the hydrogels were able to sequester the planar cationic dye, methylene blue, from solution. The structurally related hydrogels **1** and **8**, which are differentiated only by the exchange of a nitro group with a nitrile functionality, both exhibited high aspect ratio single fibres by cryo-TEM analysis, but analysis of fibres of **8** that had absorbed 20 wt% of methylene blue showed a significant decrease in fibre length and evidence of aggregation. Hydrogels **1** and **8** were able to sequester over 1 gram of dye per gram of gelator from aqueous solution, with **8** achieving high levels of dye absorption more rapidly than **1**. These structure property relationship studies will enable the realization of inexpensive and highly effective purification systems for contaminated water.

Experimental Section

Chemical characterisation: NMR spectra were recorded on either a Bruker Nano400 (9.39 T) or a Bruker DPX 400 (9.39 T) instrument, with both operating at 400 MHz or 100 MHz for ^{1}H and ^{13}C nuclei, respectively. IR spectra were recorded on a PerkinElmer Spectrum 100 FT-IR in transmission mode. All samples were analyzed as solid powders using a diamond ATR sampling accessory. Mass spectrometry was conducted using a ThermoFischer Scientific Orbitrap XL LCMS. The sample was introduced via liquid chromatography. Ionisation was achieved by electrospray ionisation (ESI). Melting points were acquired on a Stuart SMP10 melting point apparatus using a temperature ramp of 2 °C min^{-1}. UV spectra were recorded using a Varian Cary 300 Bio or a PerkinElmer Lambda 25 UV/Vis Spectrometer. Samples were analysed in quartz curettes with a 5.0 mm path length and were baseline corrected with respect to a blank cell with the appropriate solvent.

Shear rheology: Experiments were carried out using a TA Instruments AR2000 rheometer. Samples were tested in the cone-and-plate geometry using a 20 mm diameter cone. The material was analysed via frequency sweeps at low strain (1.0%).

Single-crystal X-ray diffraction: Data were collected with $Cu_{K\alpha}$ radiation on an Oxford Diffraction Gemini S Ultra CCD diffractometer equipped with an Oxford Cryosystems low-temperature device operating at 150 K. Both structures were solved by direct methods (SIR92[25]) and refined by full-matrix least squares against $|F|^2$ using all data (CRYSTALS[26]). Though all H atoms could be distinguished in the difference Fourier map, the H-atoms were included at geometrically idealized positions and refined in riding-model approximation. All full-weight non-H atoms were modelled with anisotropic displacement parameters.

Cryo-TEM: Sample preparation was carried out using a CryoPlunge 3 unit (Gatan Instruments) employing a double blot technique. A small quantity of sample was pipetted onto a plasma etched (15 s) 400 mesh holey carbon grid (Agar Scientific) held in the plunge chamber at approx 90% humidity. The samples were blotted, from both sides for around 6 s dependant on sample viscosity. The samples were then plunged into liquid ethane at a temperature of −170 °C. The grids were blotted to remove excess ethane then transferred, under liquid nitrogen to the cryo TEM specimen holder (Gatan 626 cryo holder) at −170 °C. Samples were examined using a Jeol 2100 TEM operated at 200 KV and imaged using a Gatan Ultrascan 4000 camera and images captured using DigitalMicrograph software (Gatan).

Synthesis and characterisation

General: All reagents were purchased from Sigma Aldrich and used as received without further purification. Solvents were used as supplied with the exception of THF that was distilled under argon from sodium and benzophenone prior to use. Gelator synthesis is exemplified for mono-acid hydrogelator **3**, full synthetic procedures, characterisation and NMR spectra for all new compounds are reported in the Supporting Information.

4-(3-(4-Nitrophenyl)ureido)benzoic acid (3): 4-Nitrophenylisocyanate (0.31 g, 1.90 mmol) and 4-aminobenzoic acid (0.26 g, 1.90 mmol) were dissolved in dry THF (30 mL) and stirred in an inert atmosphere for 24 h. On completion the resultant white solution was reduced in vacuo,

added dropwise to hexane (150 mL) and a pale yellow precipitate formed. The precipitate was isolated and dried to give the title compound as a pale yellow powder (0.48 g, 84 %). M.p. 241 °C (decomp); ^{1}H NMR (400 MHz, [D$_6$]DMSO): δ = 9.56 (s, 1H), 9.31 (s, 1H), 8.21 (d, 2H, J = 9.2 Hz), 7.90 (d, 2H, J = 10.8 Hz), 7.71 (d, 2H, J = 9.6 Hz), 7.58 ppm (d, 2H, J = 5.6 Hz); ^{13}C NMR (100 MHz, [D$_6$]DMSO): δ = 166.9, 151.7, 146.0, 143.2, 141.2, 130.5, 124.3, 124.0, 117.7 ppm; IR (ATR): ν = 3273, 3094, 2580, 1660, 1498, 1301, 1175, 858, 749 cm^{-1}; MS (ESI): m/z: calcd for $C_{14}H_{12}N_3O_5$: 302.0777, found 302.0722.

Crystal structure information: Crystal structure data for **3** and **5** have been deposited at the Cambridge Crystallographic Data Centre and allocated the deposition numbers: CCDC-832322, and -832323 contain the supplementary crystallographic data for this paper. These data can be obtained free of charge from The Cambridge Crystallographic Data Centre via www.ccdc.cam.ac.uk/data_request/cif.

Acknowledgements

Work in the UK was supported by EPSRC EP/G026203/1 for BWG and EPSRC for a studentship for A.L.A., a UROP studentship from the University of Reading for D.M.W. and grants from both the Diamond Light Source Ltd and the University of Reading for C.A.M. Work at Castelló was supported by MCI, grant CTQ2009-13961 and Universitat Jaume I, grants P1-1B2009-42 and P1-1B2007-11. F.R.L. thanks Generalitat Valenciana for a FPI fellowship. We acknowledge Steve Furzeland and Derek Atkins (Unilever, Colworth) for their expertise in performing the cryo-TEM experiments.

[1] a) J. W. Steed, *Chem. Commun.* **2010**, *46*, 1379–1383; b) A. R. Hirst, B. Escuder, J. F. Miravet, D. K. Smith, *Angew. Chem.* **2008**, *47*, 8002–8018; *Angew. Chem. Int. Ed.* **2008**, *120*, 8122–8139.

[2] J. M. Lehn, *Supramolecular Chemistry*, Wiley-VCH, Weinheim (Germany), **1995**.

[3] K. Murata, M. Aoki, T. Harada, H. Kawabata, T. Komri, K. Ueda, S. Shinkai, *J. Am. Chem. Soc.* **1994**, *116*, 6664–6676.

[4] a) A. R. Hirst, I. A. Coastes, T. R. Boucheteau, J. F. Miravet, B. Escuder, V. Castelletto, I. W. Hamley, D. K. Smith, *J. Am. Chem. Soc.* **2008**, *130*, 9113–9121; b) J. Chen, J. W. Kampf, A. J. McNeil, *Langmuir* **2010**, *16*, 13076–13080.

[5] P. Dastidar, *Chem. Soc. Rev.* **2008**, *37*, 2699–2715.

[6] B. Escuder, F. Rodríguez-Llansola, J. F. Miravet, *New J. Chem.* **2010**, *34*, 1044–1054.

[7] N. M. Sangeetha, U. Maitra, *Chem. Soc. Rev.* **2005**, *34*, 821–836.

[8] G. Wang, A. D. Hamilton, *Chem. Commun.* **2003**, 310–311.

[9] a) T. C. Holmes, S. de Lacalle, X. Su, A. Rich, S. Zhang, *Proc. Natl. Acad. Sci. USA* **2000**, *97*, 6728–6733; b) S. Zhang, *Nat. Biotechnol.* **2003**, *21*, 1171–1178; c) G. A. Silva, C. Czeisler, K. L. Niece, E. Beniash, D. A. Harrington, J. A. Kessler, S. I. Stupp, *Science* **2004**, *303*, 1352–1355; d) V. Jayawarna, M. Ali, T. A. Jowitt, A. E. Miller, A. Saiani, J. E. Gough, R. V. Ulijn, *Adv. Mater.* **2006**, *18*, 611–614.

[10] a) M. E. Davis, P. C. H. Hsieh, T. Takahashi, Q. Song, S. Zhang, R. D. Kamm, A. J. Grodzinsky, P. Anversa, R. T. Lee, *Proc. Natl. Acad. Sci. USA* **2006**, *103*, 8155–8160; b) V. F. M. Segers, R. T. Lee, *Drug Discovery Today* **2007**, *12*, 561–568; c) M. C. Branco, D. J. Pochan, N. J. Wagner, J. P. Schneider, *Biomaterials* **2009**, *30*, 1339–1347; d) F. Gelain, L. D. Unsworth, S. Zhang, *J. Contr. Release* **2010**, *145*, 231–239.

[11] For example see: a) S. Bhattacharya, Y. Krishnan-Ghosh, *Chem. Commun.* **2001**, 185–186; b) B. Adhikari, G. Palui, A. Banerjee, *Soft Matter* **2009**, *5*, 3452; c) J. Wang, H. Wang, Z. Song, D. Kong, X. Chen, B. Z. Yang, *Colloids Surf. B* **2010**, *80*, 155–160.

[12] F. Rodríguez-Llansola, B. Escuder, J. F. Miravet, D. Hermida-Merino, I. W. Hamley, C. J. Cardin, W. Hayes, *Chem. Commun.* **2010**, *46*, 7960–7962.

[13] For recent examples of non-peptidic, non-metal binding urea based molecular hydrogels see: a) D. Krishna Kumar, D. Amilan Jose, A. Das, P. Dastidar, *Chem. Commun.* **2005**, 4059–4061; b) M. Yamanaka, T. Nakamura, T. Nakagawa, H. Itagaki, *Tetrahedron Lett.* **2007**, *17*, 8990–8993; c) M. Yamanaka, T. Nakagawa, R. Aoyama, T. Nakamura, *Tetrahedron* **2008**, *64*, 11558–11567; d) G. O. Lloyd, J. W. Steed, *Soft Matter* **2011**, *7*, 75–84.

[14] V. Prévost, L. M. Qian, O. Ruel, E. Perez, *J. Am. Chem. Soc.* **2001**, *123*, 8177–8188.

[15] D. J. Adams, M. F. Butler, W. J. Frith, M. Kirkland, L. Mullen, P. Sanderson, *Soft Matter* **2009**, *5*, 1856–1862.

[16] For examples of metastable gels see: a) Y. Wang, L. Tang, J. Yu, *Cryst. Growth Des.* **2008**, *8*, 884–889; b) J. R. Moffat, D. K. Smith, *Chem. Commun.* **2008**, *44*, 2248–2250; c) D. J. Adams, K. Morris, L. Chen, L. C. Serpell, J. Bacsa, G. M. Day, *Soft Matter* **2010**, *6*, 4144–4156; d) P. Zhu, X. Yan, Y. Su, Y. Yang, J. Li, *Chem. Eur. J.* **2010**, *16*, 3176–3183; e) D. Gräbner, L. Zhai, I. Talmon, O. Glatter, B. Herzog, H. Hoffmann, *J. Phys. Chem. B* **2008**, *112*, 2901–2908.

[17] We have previously observed that hydrogel **1** formed rapidly through an HCl pH switch was also stable to above 100 °C. See ref. [12].

[18] E. Pretsch, P. C. Affolter, *Structure Determination of Organic Compounds: Tables of Spectral Data*, Springer, **2000**.

[19] For examples of dye absorbing molecular hydrogelators see: a) S. Ray, A. K. Das, A. Banerjee, *Chem. Mater.* **2007**, *19*, 1633–1639; b) S. Debnath, A. Shome, S. Dutta, P. K. Das, *Chem. Eur. J.* **2008**, *14*, 6870–6881; c) T. Kar, S. Debnath, D. Das, A. Shome, P. K. Das, *Langmuir* **2009**, *25*, 8639–8648; d) S. Dutta, D. Das, A. Dasgupta, P. K. Das, *Chem- Eur. J.* **2010**, *16*, 1493–1505.

[20] a) B. L. A. Estroff, L. Leiserowitz, L. Addadi, S. Weiner, A. D. Hamilton, *Adv. Mater.* **2003**, *15*, 38–42; b) H. Cui, T. K. Hodgdon, E. W. Kaler, L. Abezgauz, D. Danino, M. Lubovsky, Y. Talmon, D. J. Pochan, *Soft Matter* **2007**, *3*, 945–955.

[21] a) V. Castelletto, G. Cheng, B. W. Greenland, I. W. Hamley, P. J. F. Harris, *Langmuir* **2011**, *27*, 2980–2988; b) G. Cheng, V. Castelletto, R. R. Jones, C. J. Connon, I. W. Hamley, *Soft Matter* **2011**, *7*, 1326–1333; c) K. M. Galler, L. Aulisa, K. R. Regan, R. N. D'Souza, J. D. Hartgerink, *J. Am. Chem. Soc.* **2010**, *132*, 3217–3223; d) S. E. Paramonov, H.-W. Jun, J. D. Hartgerink, *J. Am. Chem. Soc.* **2006**, *128*, 7291–7298; e) R. A. Hule, R. P. Nagarkar, A. Altunbas, H. R. Ramay, M. C. Branco, J. P. Schneider, D. J. Pochan, *Faraday Discuss.* **2008**, *139*, 251–264; f) R. A. Hule, R. P. Nagarkar, B. Hammouda, J. P. Schneider, D. J. Pochan, *Macromolecules* **2009**, *42*, 7137–7145.

[22] E. Krieg, E. Shirman, H. Weissman, E. Shimoni, S. G. Wolf, I. Pinkas, B. Rybtchinski, *J. Am. Chem. Soc.* **2009**, *131*, 14365–14373.

[23] a) M. C. Etter, Z. Urbañcyzk-Lipkowska, *J. Am. Chem. Soc.* **1988**, *110*, 5896–5897; b) L. S. Reddy, S. K. Chandra, S. George, N. J. Badu, A. Nangia, *Cryst. Growth Des.* **2007**, *7*, 2675–2690; c) R. Custelcean, *Chem. Commun.* **2008**, 295–307.

[24] The propensity for related structure to crystallise with $Z' > 1$ remains a debated topic, see: a) K. M. Anderson, A. E. Goeta, J. W. Steed, *Cryst. Growth Des.* **2008**, *8*, 2517–2524; b) G. R. Desiraju, *CrystEngComm* **2007**, *9*, 91–92.

[25] A. Altomare, G. Cascarano, C. Giacovazzo, A. Guagliardi, M. C. Burla, G. Polidori, M. Camalli, *J. Appl. Crystallogr.* **1994**, *27*, 435.

[26] P. W. Betteridge, J. R. Carruthers, R. I. Cooper, K. Prout, D. J. Watkin, *J. Appl. Crystallogr.* **2003**, *36*, 1487.

Received: July 12, 2011
Revised: October 21, 2011
Published online: January 26, 2012

